Electronic Supplementary Material (ESI) for Analyst.
This journal is © The Royal Society of Chemistry 2024

Supporting Information

Spectroelectrochemical Determination of Thiolate Self-Assembled Monolayer Adsorptive Stability in Aqueous and Non-Aqueous Electrolytes

Abdur-Rahman Siddiqui [a±], Jeanne N'Diaye [a, b±], Armando Santiago Carboney [a±], Kristin Martin[a], Rohit Bhargava [b, c], and Joaquín Rodríguez-López [a, b*]

[a] Department of Chemistry, University of Illinois Urbana-Champaign, Urbana, Illinois, 61801, USA

[b] The Beckman Institute for Advanced Science and Technology, University of Illinois Urbana-Champaign, Urbana, Illinois 61801, USA

[c] Department of Bioengineering, University of Illinois Urbana-Champaign, Urbana, Illinois 61801, United States

[±]: The authors contributed equally.

Table of Contents

Supplementary Figures, Tables, and Schemes……..……....S3

Figure S1: Reductive Desorption Curves of each SAM…….……...……S3

Scheme S1: Schematics of the custom-built static SPR cell…….…….……...S3

Figure S2: CVs of 4-PySH cycled outside and within SPW…….…….……...S4

Figure S3: Spectra of 4-NTP at applied potentials…..…….……...……...……S4

Figure S4: CVs of 4-PySH cycled at 1 mV/s in KOH and $HClO_4$……...……....……S5

Table S1: The pKa of each SAM used in the study…….…….....S5

Figure S5: SPR Sensorgrams of the Aqueous systems…….……...……...……S5

Figure S6: CVs of the SPW of the Aprotic Solvents …….……...S6

Figure S7: CVs of Bare Gold and SAM-covered Electrodes in Aprotic Solvents ……...S6

Figure S8: CVs of the SPW of the Alcohols…….. …….……S7

Table S2: Comparing the SPW Size to Polarity Index of Non-Aqueous Solvents …….....S7

Figure S9: SEIRAS Spectra of 4-MA in the Aprotic Solvents…….…….....S8

Scheme S2: Proposed Potential-Induced Configuration Change of SAMs…….……..…S8

Figure S10: Spectra of 4-MA in BuOH undergoing conformation changes…...……..……S9

Figure S11: SPR Sensorgrams of the Alcohols…….……..…..…S9

Figure S12: SPR Sensorgrams of the Aprotic Solvents …….……...……...……..…S10

Figure S13: CVs of Bare Gold and SAM-covered Electrodes in using SEIRAS chip ……...S10

Figure S14: CVs of each SAM for 50 Cycles in 1M KOH……..……...S11

Figure S16: CVs of each SAM for 50 Cycles in 0.1M NaCl……..…….....S11

Figure S17: CVs of each SAM for 50 Cycles in 0.1M $HClO_4$…….……...S12

Figure S18: CVs of each SAM for 50 Cycles in 0.1M LiCl MeOH……...S12

Figure S19: CVs of each SAM for 50 Cycles in 0.1M LiCl EtOH……..……...S13

Figure S20: CVs of each SAM for 50 Cycles in 0.1M LiCl IPA…..……...S13

Figure S21: CVs of each SAM for 50 Cycles in 0.1M LiCl BuOH.…….....S14

Figure S21: CVs of each SAM for 50 Cycles in 0.1M $TBAPF_6$ MeCN.……...S14

Figure S22: CVs of each SAM for 50 Cycles in 0.1M $TBAPF_6$ PC...…….....S15

Figure S23: CVs of each SAM for 50 Cycles in 0.1M $TBAPF_6$ DMF...……...S15

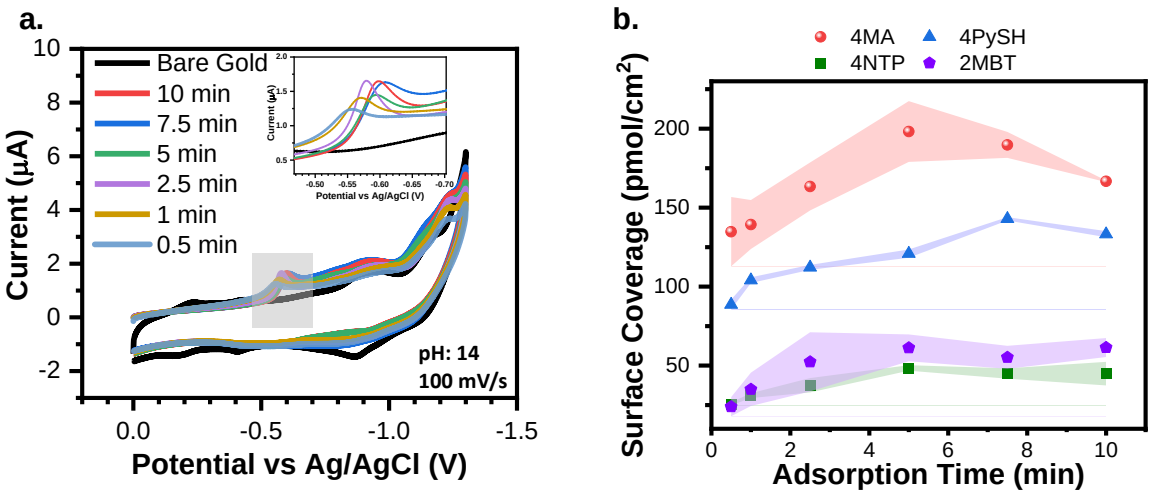

Figure S1: (a) Reductive desorption CVs of a gold electrode soaked in 1 mM 4-PySH for different times in 1 M KOH. **(b)** A plot of the calculated surface coverage of each SAM at different adsorption times from 0.5, 1, 2.5, 5, 7.5, and 10 minutes.

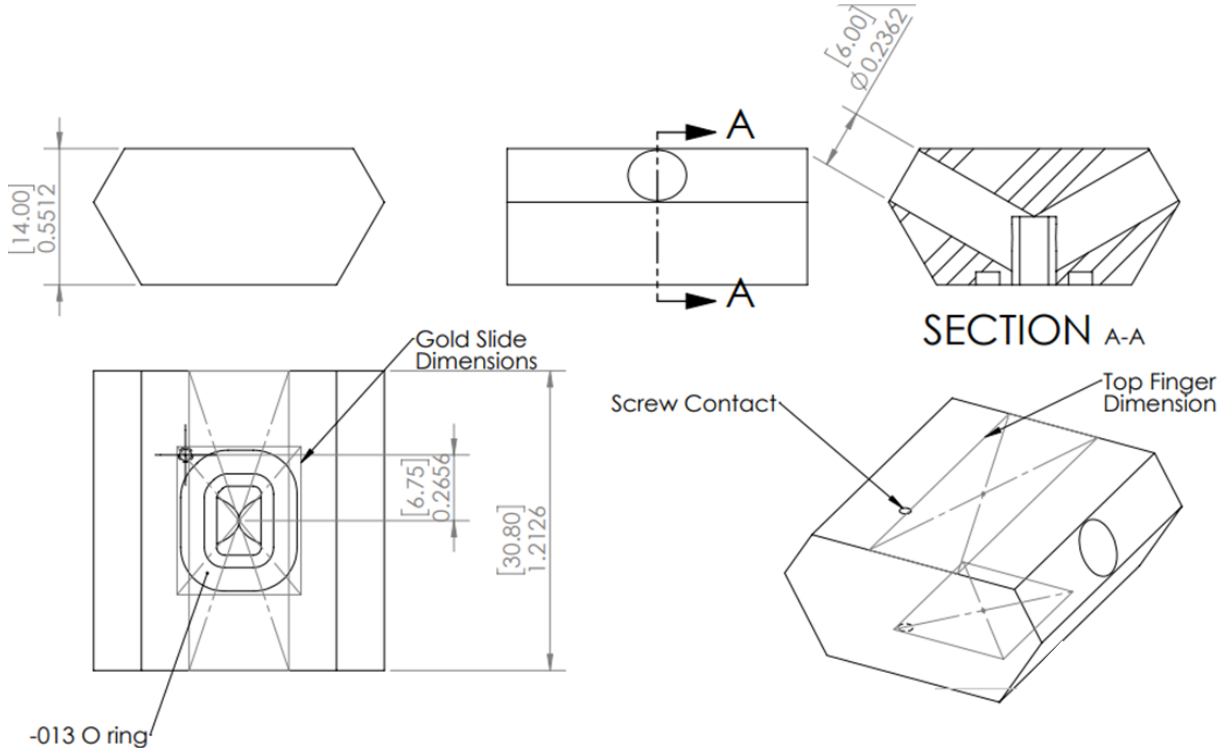

Scheme S1: Schematic of the custom-built static SPR cell. The cell went over the prism used in the SPR. Copper tape was used for electrochemical contact with gold sensor chip. There are two openings on the sides allowing the addition of electrolytes solutions, reference and counter electrodes.

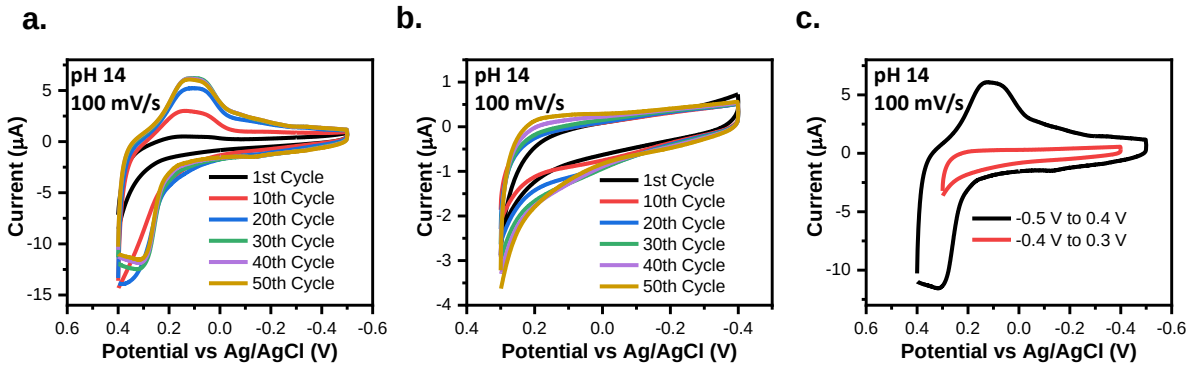

Figure S2: CV of a 4-PySH-covered electrode in 1 M KOH when cycling between **(a)** -0.5 V and 0.4 V or **(b)** -0.4 V and 0.3 V for 50 cycles. **(c)** Comparing the 50th cycle of the CVs in **(a)** and **(b)**.

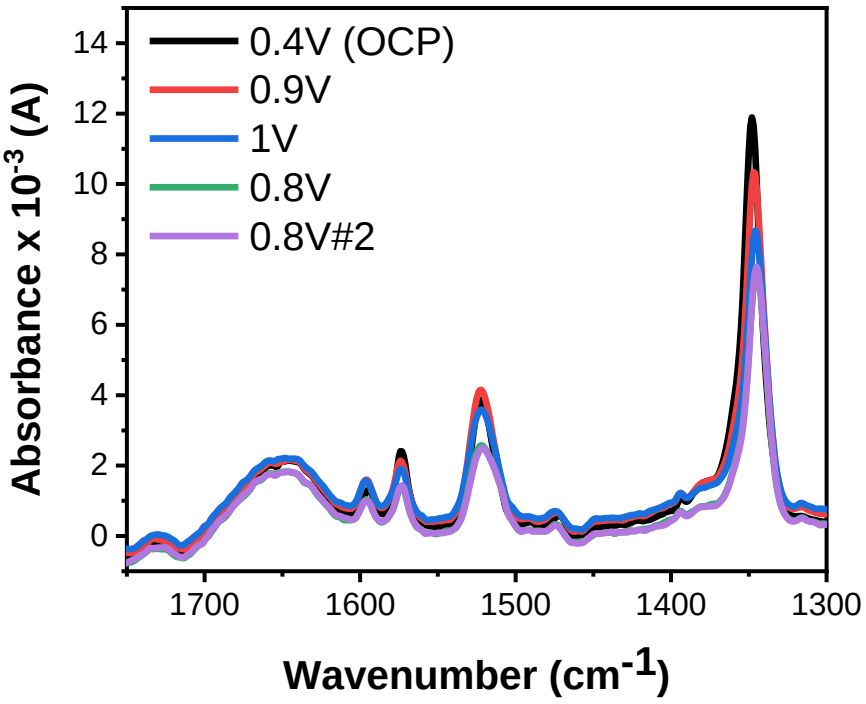

Figure S3: Spectra of a 4-NTP modified SEIRAS substrate at different applied potentials within 0.1 M $HClO_4$. The spectra were attained in descending order of the legend.

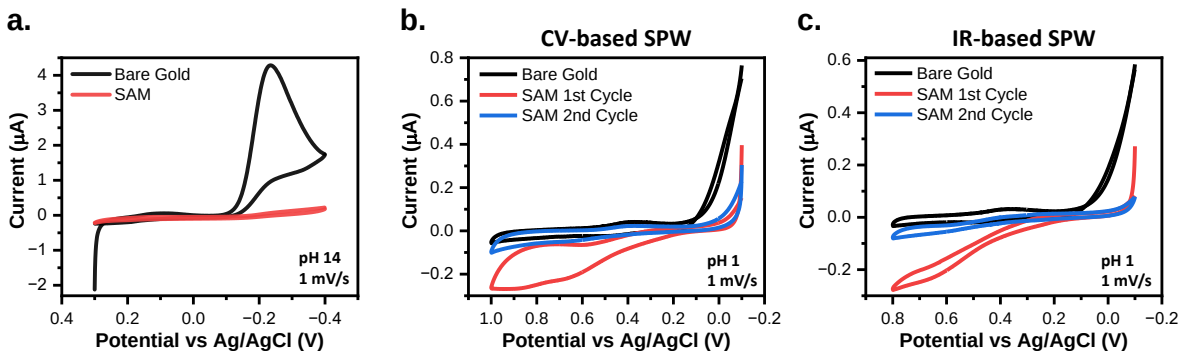

Figure S4: CVs 4-PySH modified electrodes compared to baseline CVs cycled within the CV and IR-based SPWs established for **(a)** 1 M KOH **(b-c)** 0.1 M $HClO_4$

Table S1: The reported pKa of 4MA, 4-NTP, 4-PySH, and 2-MBT.

SAM	pKa
4-MA	8.74
4-NTP	4.68
4-PySH	1.43
2-MBT	9.80

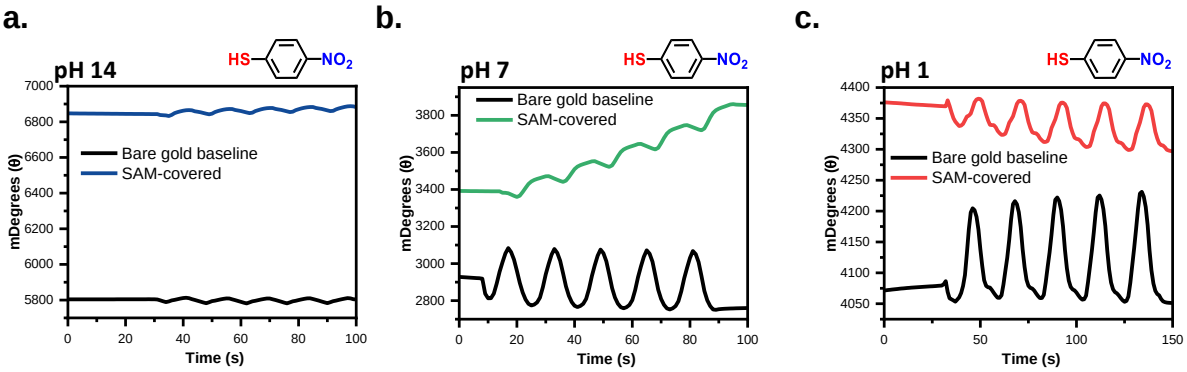

Figure S5: Sensorgrams of a 4-NTP modified SPR Au chip within the SPW window as identified by bulk and SEIRAS measurements at varied pH **(a)** 1 M KOH (pH 14), **(b)** 0.1 M NaCl (pH 7), and **(c)** 0.1 M HClO4 (pH 1).

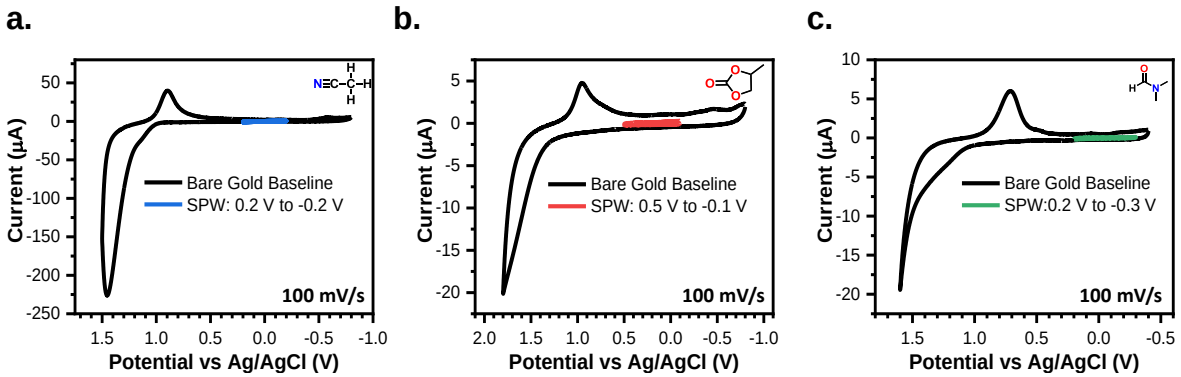

Figure S6: CVs of a bare gold electrode compared to a 4-MA-covered electrode cycled within the SPW in 0.1M $TBAPF_6$ **(a)** MeCN, **(b)** PC, and **(c)** DMF.

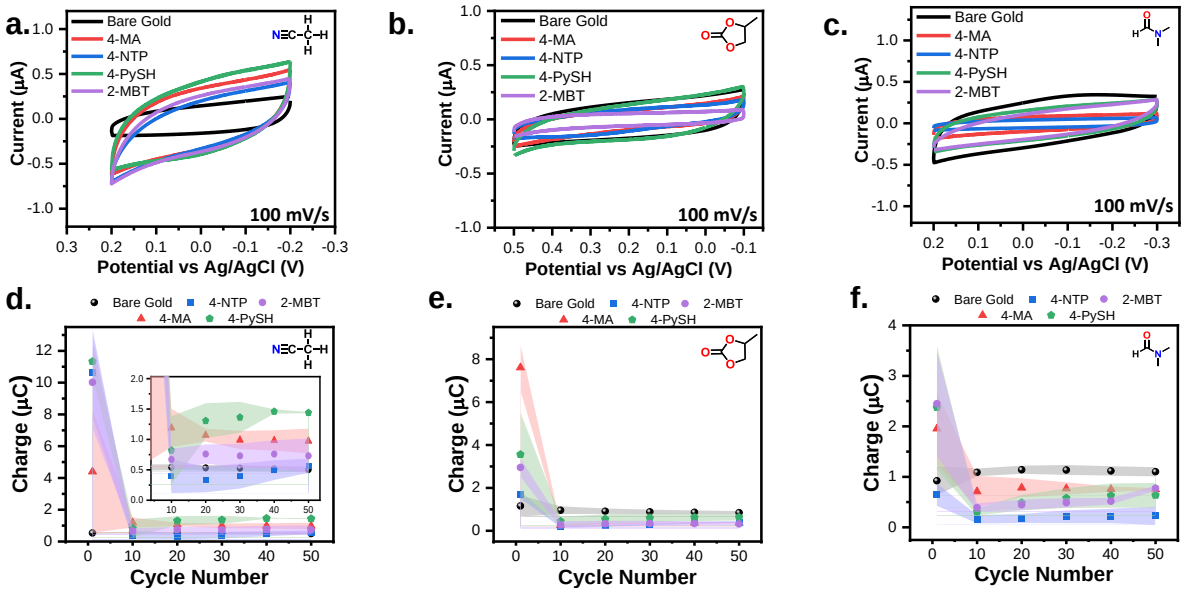

Figure S7: CVs of a bare gold electrode and SAM covered electrode in 0.1M $TBAPF_6$ **(a)** MeCN, **(b)** PC, **(c)** DMF The calculated charge of a bare gold electrode and the SAM covered electrodes at different cycle numbers when cycled in the operation window for 50 cycles in **(d)** MeCN (insert showing in zoomed region between 10-50 cycles), **(e)** PC, **(f)** DMF. The shaded regions depict the standard deviation of each measurement for three independent measurements.

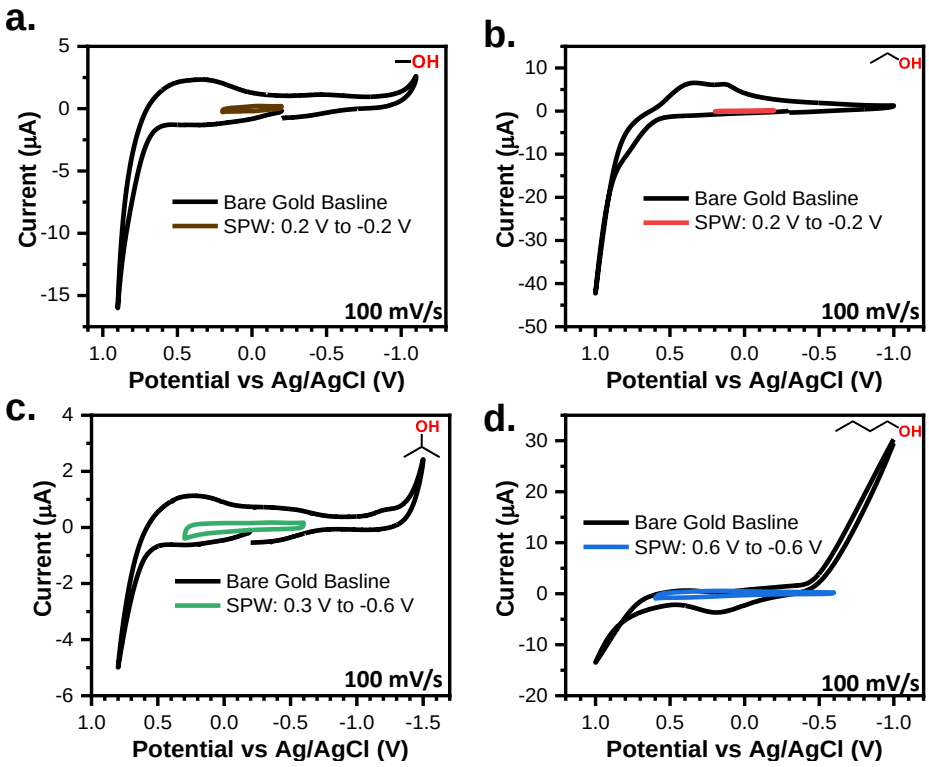

Figure S8: CVs of a bare gold electrode compared to a 4-MA-covered electrode cycled within the SPW in 0.1 M LiCl **(a)** MeOH, **(b)** EtOH, **(c)** IPA, and **(d)** BuOH.

Table S2: Comparing the SPW with the polarity index of each non-aqueous solvent.

Solvent	CV-based SPW (mV)	IR-Based SPW (mV)	Polarity Index
DMF	600	300	6.4
PC	500	500	6.1
MeCN	400	400	5.8
MeOH	400	300	5.1
EtOH	400	400	4.3
IPA	900	900	4.0
BuOH	1200	1000	3.9

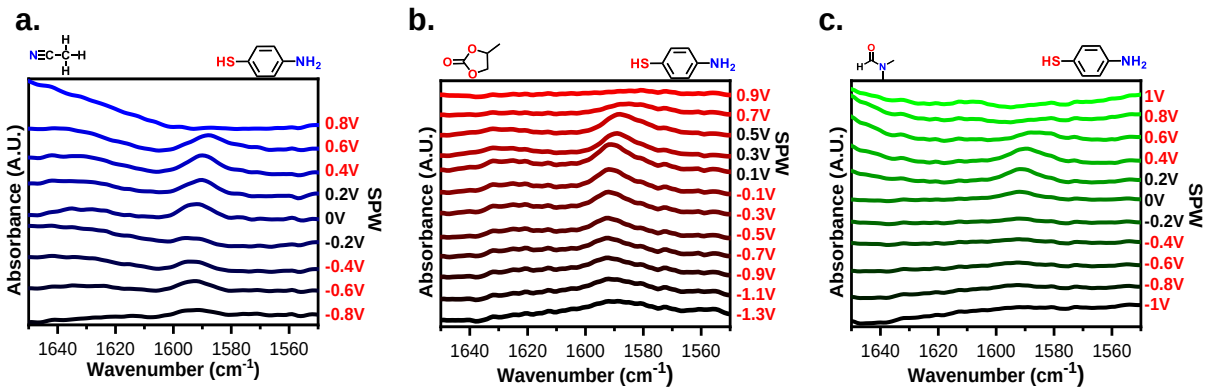

Figure S9: The potential-dependence SEIRAS spectra of 4-Mercaptoaniline (4-MA) on a gold-plated internal IRE in **(a)** MeCN, **(b)** PC, **(c)** DMF.

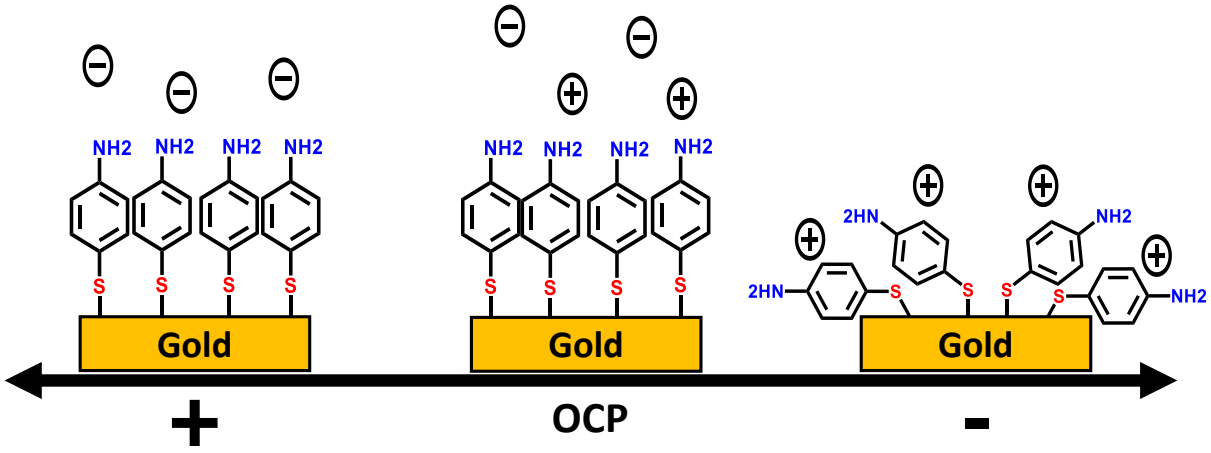

Scheme S2: Proposed scheme for the conformation change of the SAM induced by applied potential.

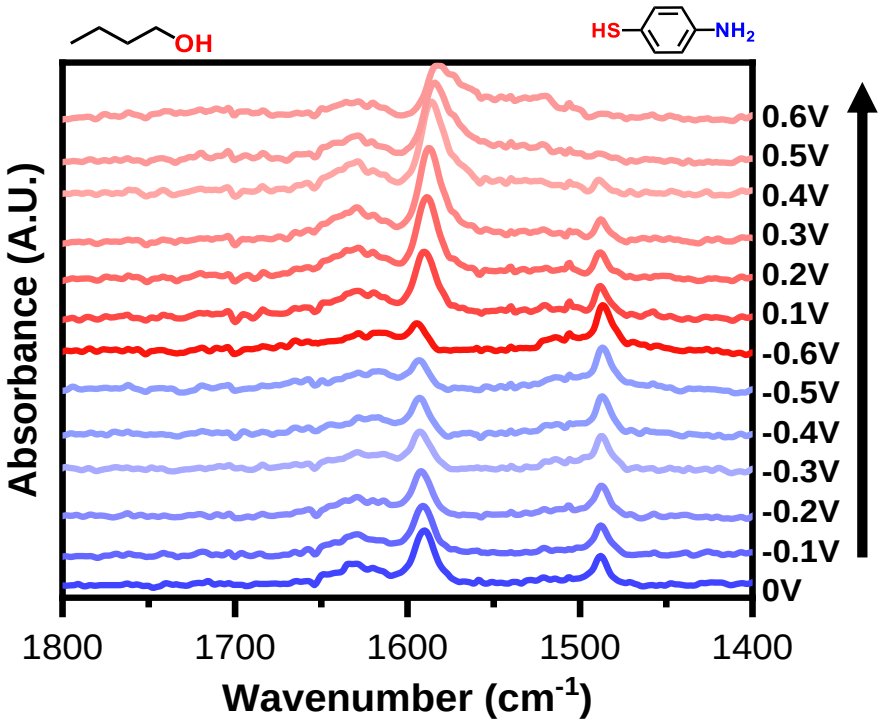

Figure S10: Potential-dependent SEIRAS spectra of 4-MA on a gold-plated internal IRE in 0.1 M LiCl BuOH within the SPW. The spectra were taken from 0 V to -0.6V and then immediately from 0.1 V to 0.6 V.

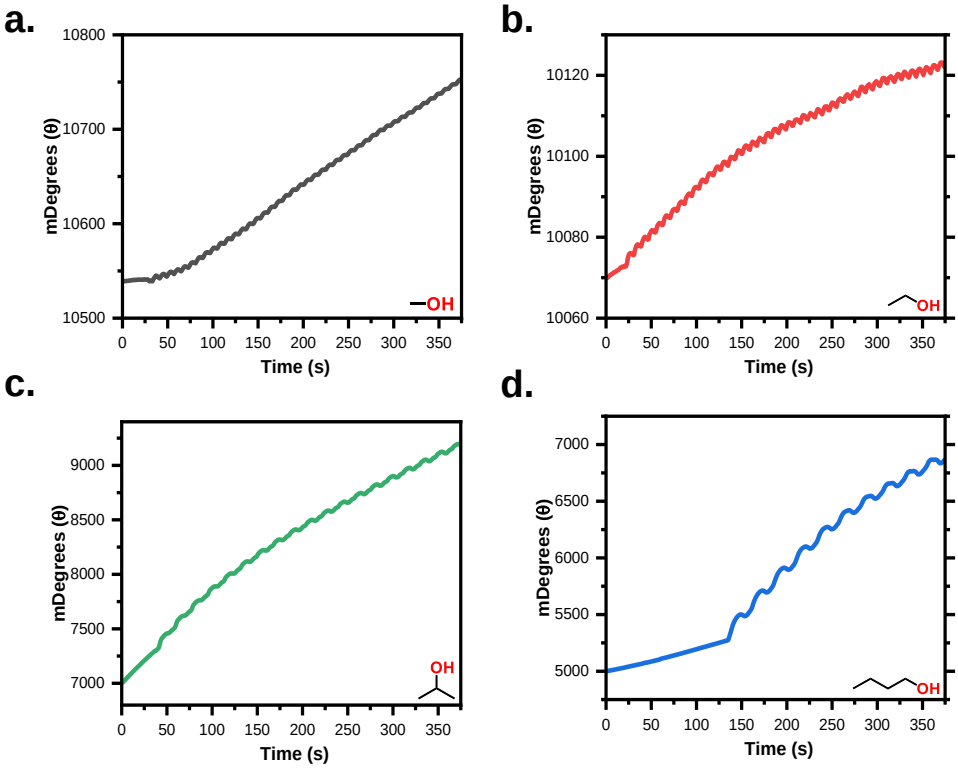

Figure S11: Sensorgrams of a 4-MA modified SPR Au chip cycled within the CV-based SPWs in 0.1 M LiCl (a) MeOH, (b) EtOH (c) IPA, and (d) BuOH.

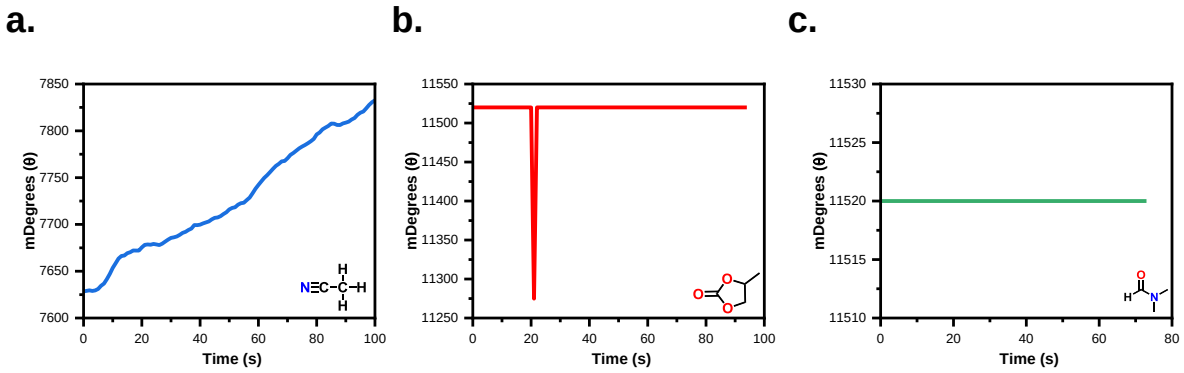

Figure S12: Sensorgrams of a 4-MA modified SPR Au chip cycled within the CV-based SPWs in 0.1 M $TBAPF_6$ **(a)** MeCN, **(b**) PC, **(c)** DMF.

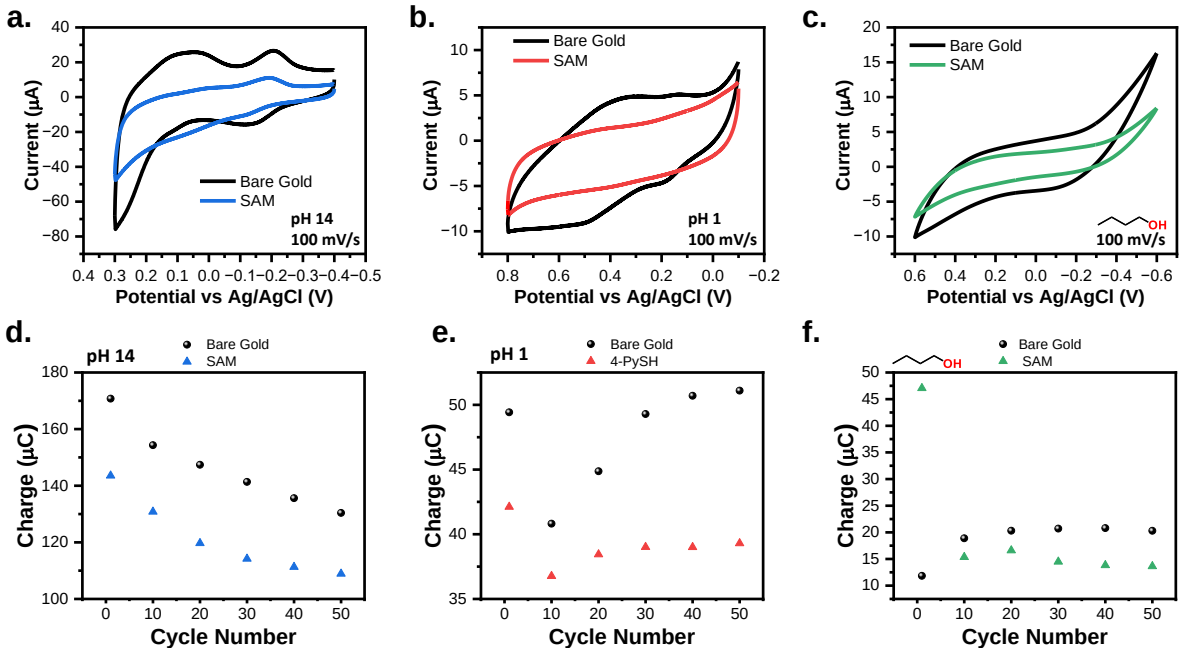

Figure S13: CVs of 4-PySH modified electrodeposited SEIRAS Au chip electrodes compared to baseline CVs cycled within the SPWs established for **(a)** 1 M KOH, **(b)** 0.1 M $HClO_4$, and **(c)** 0.1 M LiCl BuOH. The integrated charge from the anodic sweeps of the baseline and modified electrodes CVs **(a-c)** are plotted versus the cycle number in **(d)** KOH, **(e)** $HClO_4$, and **(f)** BuOH.

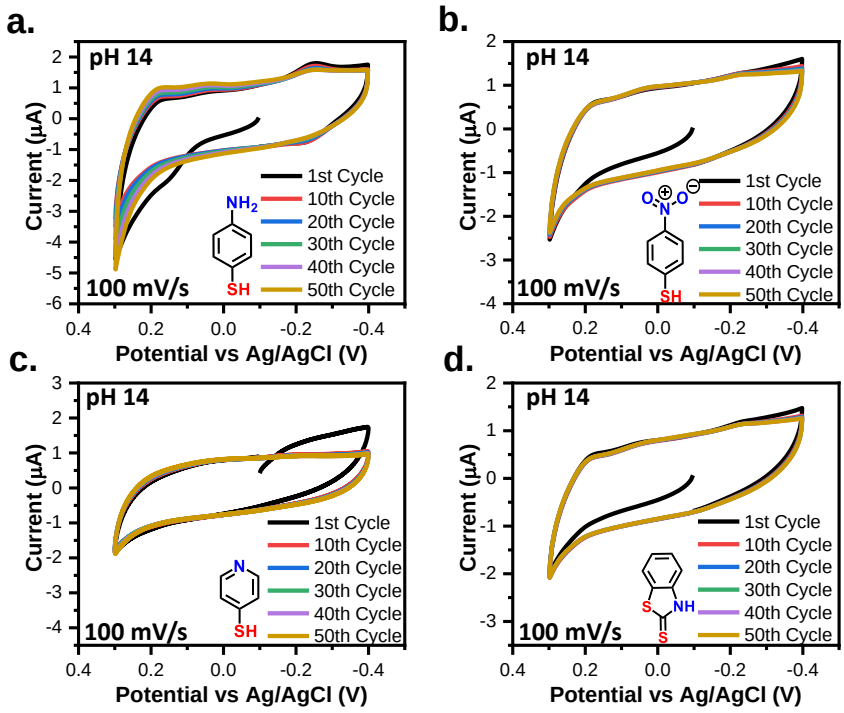

Figure S14: The CV of every 10 cycles during a stability test of 50 cycles for **(a)** 4MA, **(b)** 4NTP, **(c)** 4PySH, and **(d)** 2MBT in 1 M KOH.

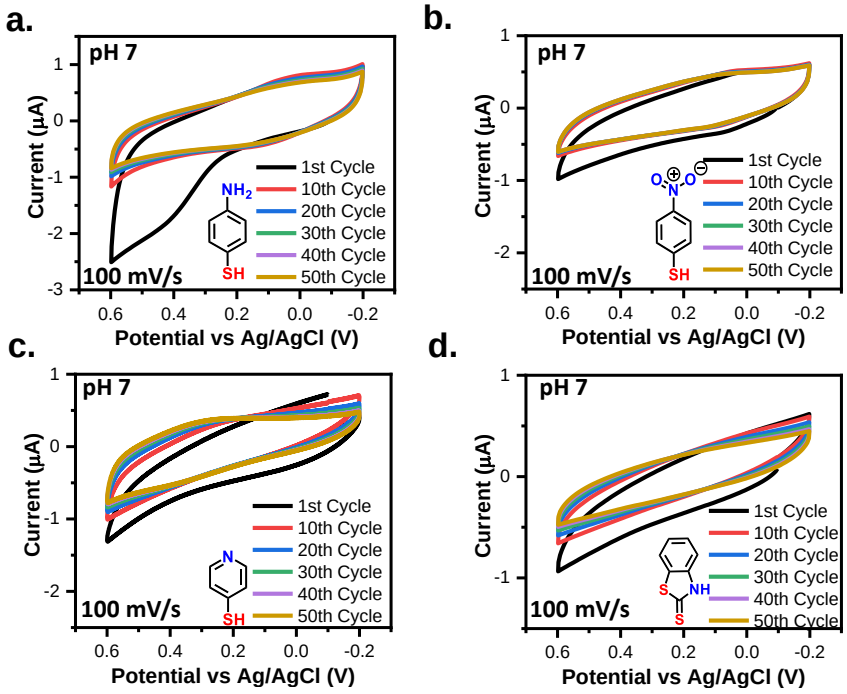

Figure S15: The CV of every 10 cycles during a stability test of 50 cycles for **(a)** 4MA, **(b)** 4NTP, **(c)** 4PySH and **(d)** 2MBT in 0.1 M NaCl.

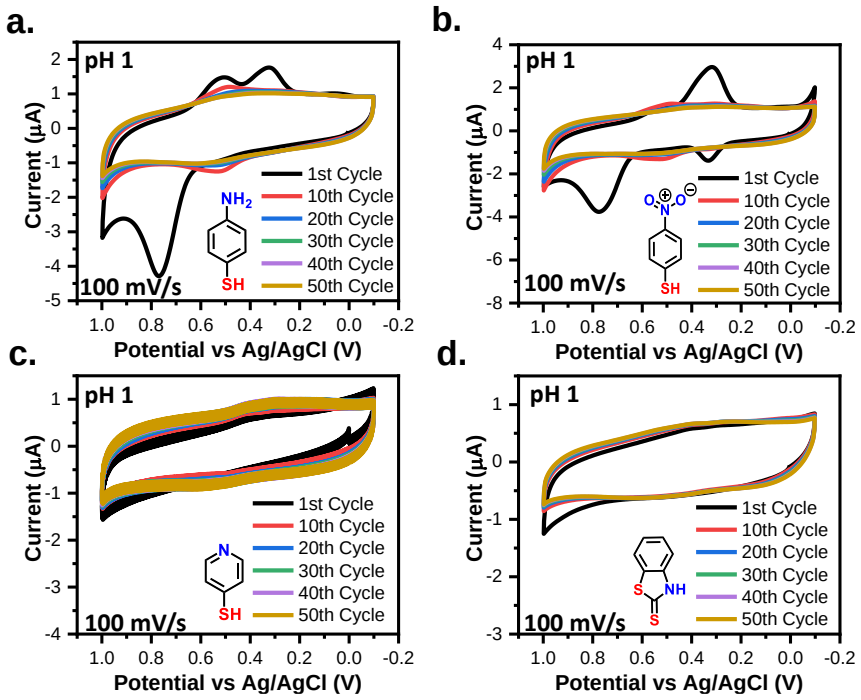

Figure S16: The CV of every 10 cycles during a stability test of 50 cycles for **(a)** 4MA, **(b)** 4NTP, **(c)** 4PySH and **(d)** 2MBT in 0.1 M $HClO_4$.

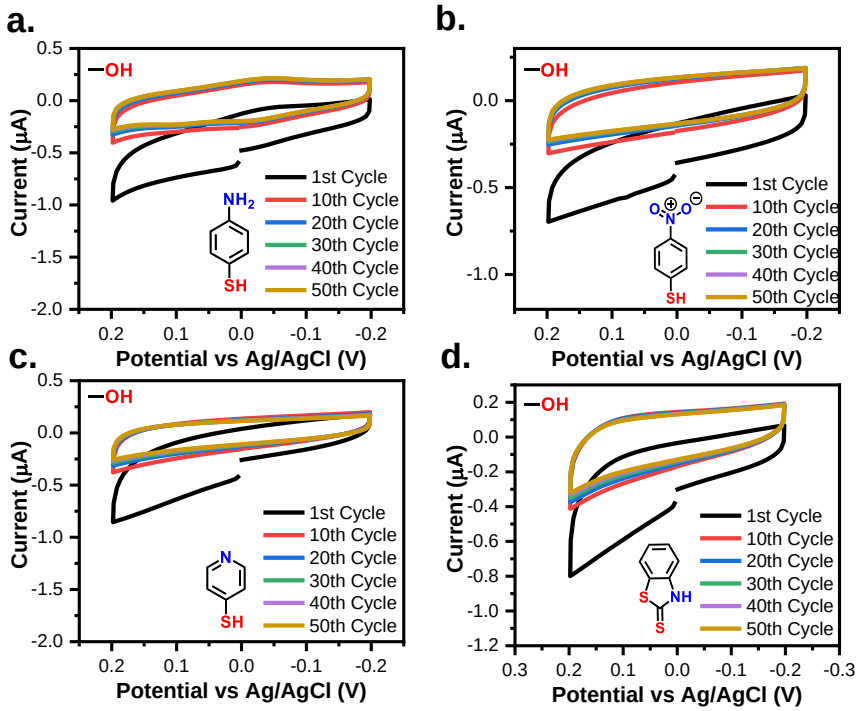

Figure S17: The CV of every 10 cycles during a stability test of 50 cycles for **(a)** 4MA, **(b)** 4NTP, **(c)** 4PySH and **(d)** 2MBT in 0.1 M LiCl methanol.

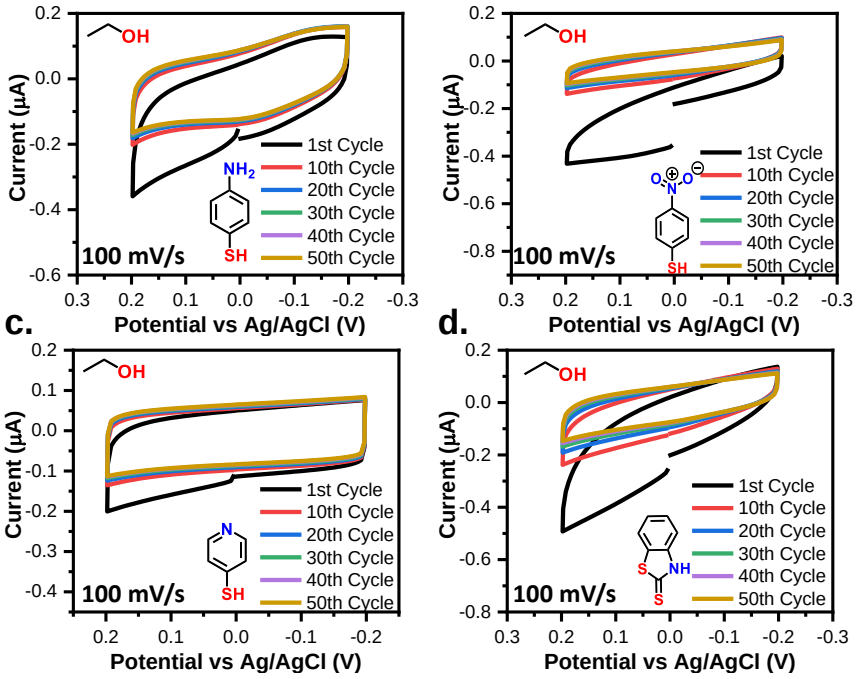

Figure S18: The CV of every 10 cycles during a stability test of 50 cycles for **(a)** 4MA, **(b)** 4NTP, **(c)** 4PySH and **(d)** 2MBT in 0.1 M LiCl ethanol.

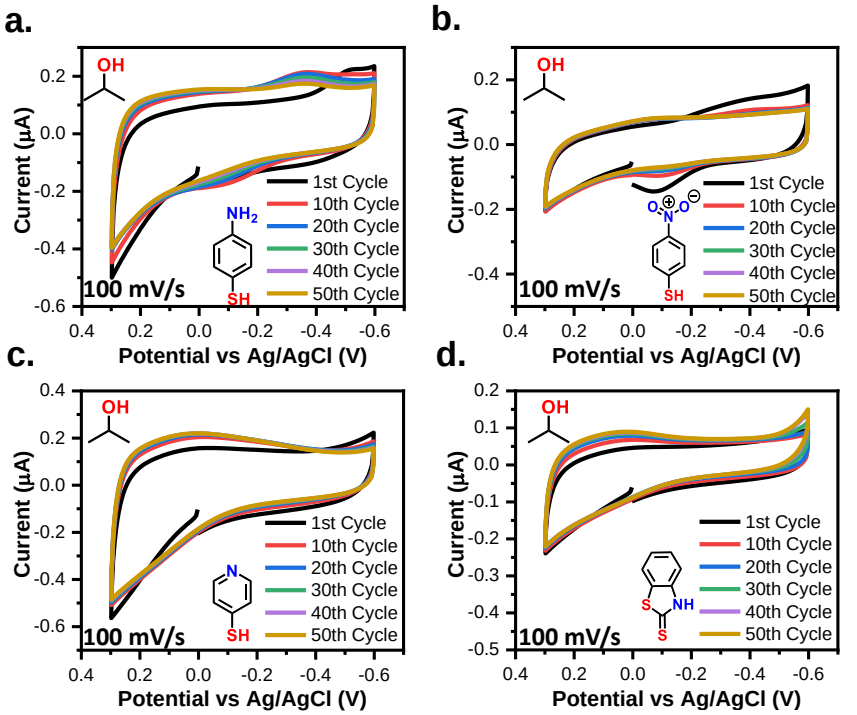

Figure S19: The CV of every 10 cycles during a stability test of 50 cycles for **(a)** 4MA, **(b)** 4NTP, **(c)** 4PySH and **(d)** 2MBT in 0.1 M LiCl propanol.

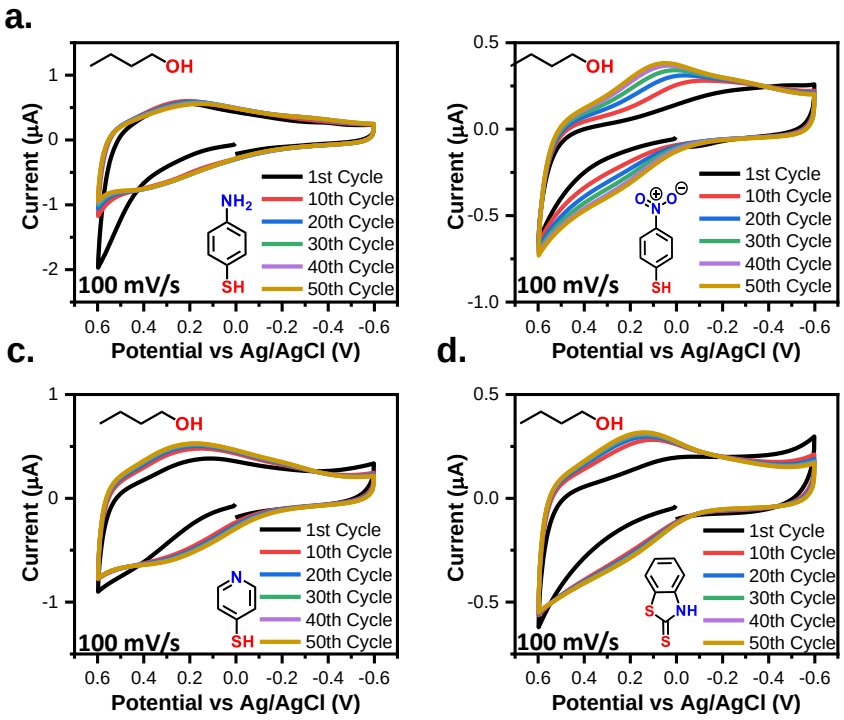

Figure S20: The CV of every 10 cycles during a stability test of 50 cycles for **(a)** 4MA, **(b)** 4NTP, **(c)** 4PySH and **(d)** 2MBT in 0.1 M LiCl butanol.

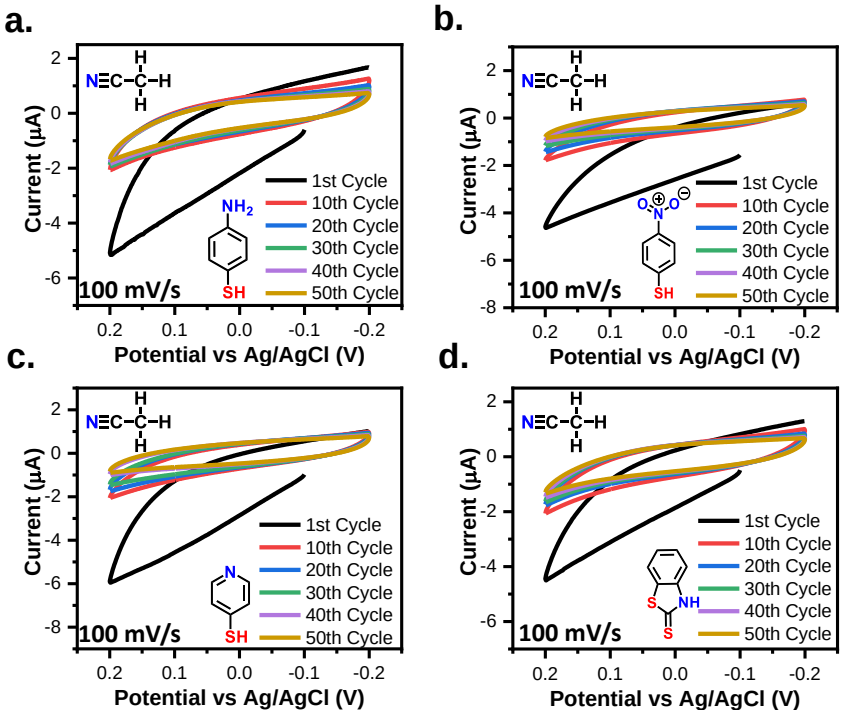

Figure S21: The CV of every 10 cycles during a stability test of 50 cycles for **(a)** 4MA, **(b)** 4NTP, **(c)** 4PySH and **(d)** 2MBT in 0.1 M $TBAPF_6$ MeCN.

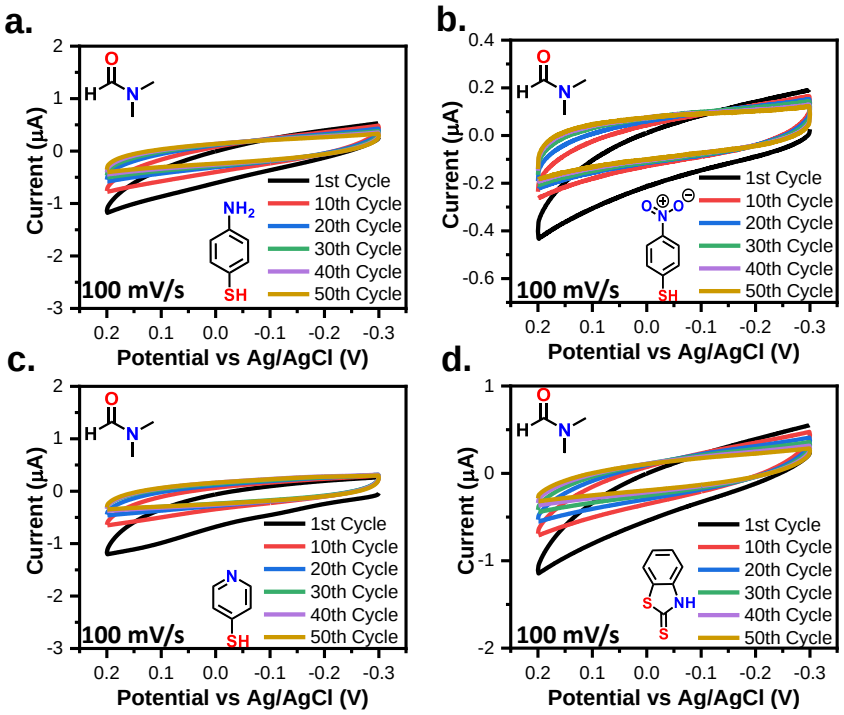

Figure S22: The CV of every 10 cycles during a stability test of 50 cycles for **(a)** 4MA, **(b)** 4NTP, **(c)** 4PySH and **(d)** 2MBT in 0.1 M $TBAPF_6$ DMF.

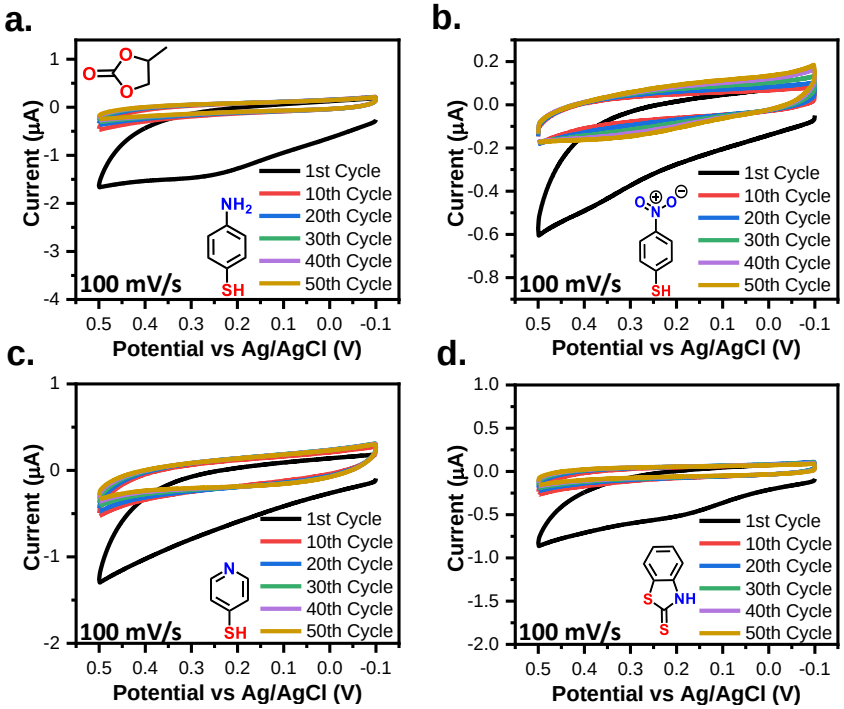

Figure S23: The CV of every 10 cycles during a stability test of 50 cycles for **(a)** 4MA, **(b)** 4NTP, **(c)** 4PySH and **(d)** 2MBT in 0.1 M $TBAPF_6$ PC.